

Supporting Information

Solvents dependent reactivities of di-, tetra- and hexanuclear manganese complexes: syntheses, structures and magnetic properties

Hua Yang,^a Fan Cao,^b Dacheng Li,^a Suyuan Zeng,^a You Song,^{*,b} and Jianmin Dou^{*,a}

Received (in XXX, XXX) Xth XXXXXXXXXX 20XX, Accepted Xth XXXXXXXXXX 20XX

DOI: 10.1039/b000000x

Contents:

Scheme S1 The possible reaction process of complexes **1–5** with the original ligand undergoing in situ reaction in different solvents.

Fig. S1. UV-vis spectra

Fig. S2. Thermogravimetric Analysis

Fig. S3 The 3D packing arrangement of **1** formed through C–H···O supramolecular interactions.

Fig. S4 The 3D packing arrangement of **2** formed through C–H···O supramolecular interactions.

Fig. S5 The 3D packing arrangement of **3** formed through C–H···O supramolecular interactions.

Fig. S6 The 3D packing arrangement of **5** formed through C–H···O supramolecular interactions.

Fig. S7 The spin states of complex **3** and magnetic exchange paths.

Fig. S8 Plots of isothermal magnetization M versus field H for complex **5** between 1.8–5 K.

Fig. S9 Plots of reduced magnetization M versus H/T at the indicated applied fields.

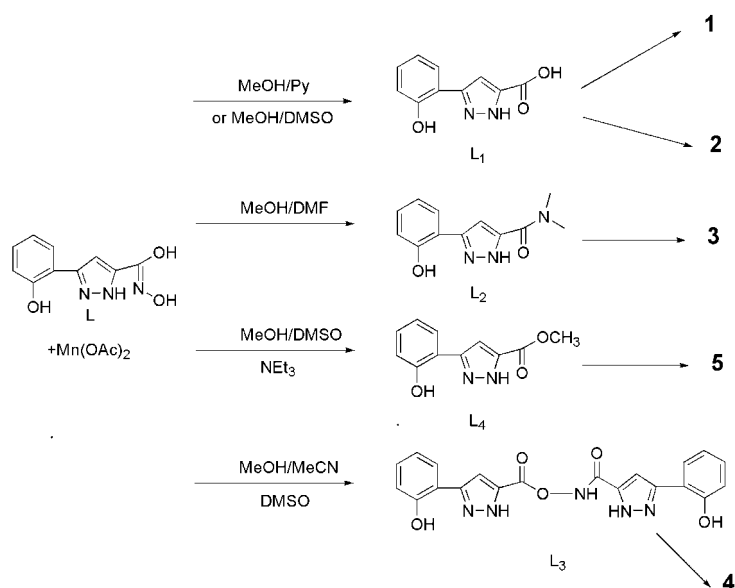
Fig. S10 The local spin in each triangular aza8-MC-3 subunit.

Table S1 Selected bond distances (Å) and angles (°) for complexes **1–3** and **5**.

Table S2 The supramolecular interactions in complexes **1–3** and **5**.

Theoretical Model for complex 3.

The magnetic susceptibility of complex 5.



Scheme S1. The possible reaction process of complexes **1–5** with the original ligand undergoing in situ reaction in different solvents.

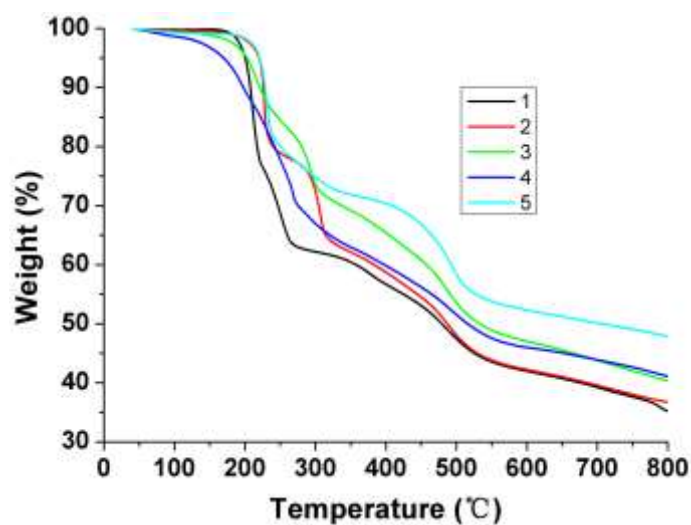


Fig. S1. TGA plots of complexes **1–5**.

The TGA curves of complexes **1–5** display different weight loss. The weight loss began from 200–300°C and corresponded to the loss of the coordination solvent molecules. Upon further heating, the organic frameworks collapse to form metal oxide components.

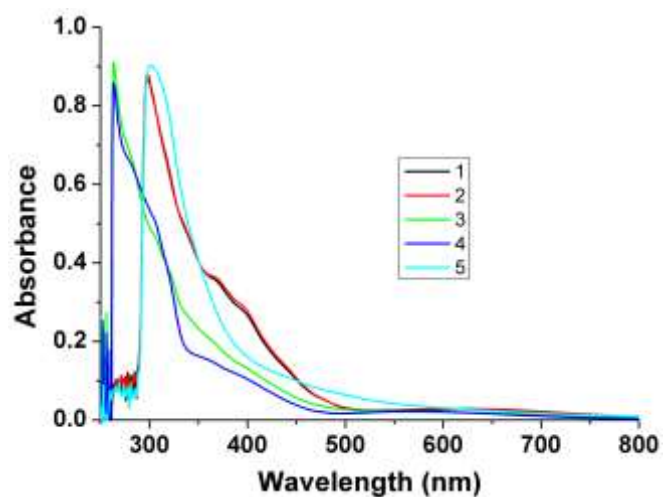


Fig. S2. UV-vis spectra for complexes **1–5** in DMF.

The UV-vis absorption spectra of complexes 1–5 dissolved in DMF exhibit two kinds of different characteristic absorption bands. Complexes 1, 2 and 5 present the same adsorption bands at 300 nm, while the adsorption peaks were observed for complex 3 and 4 at 263nm.

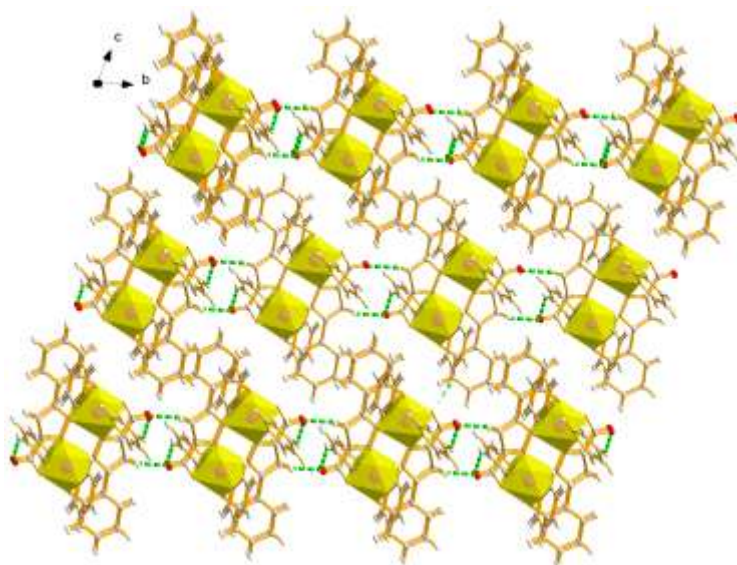


Fig. S3. Three-dimensional framework via supramolecular interactions of complex **1**.

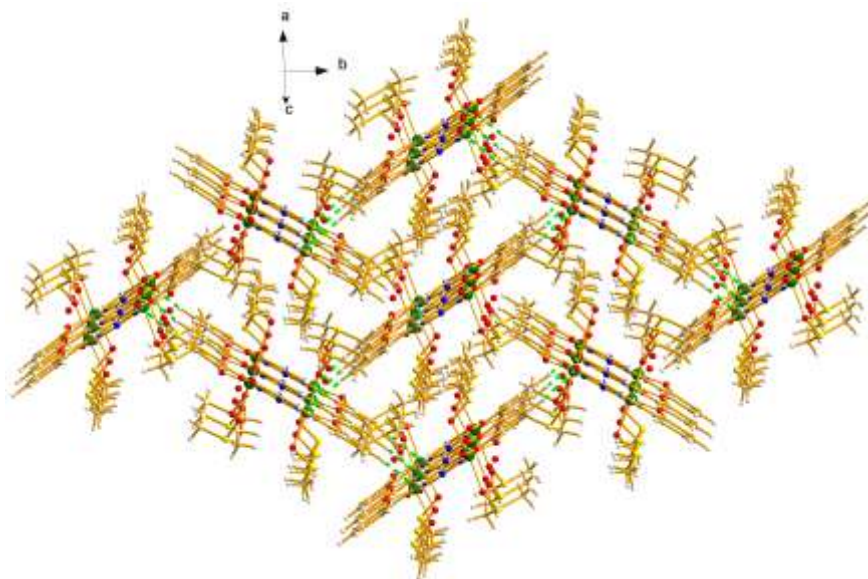


Fig. S4. Three-dimensional framework via supramolecular interactions of complex **2**.

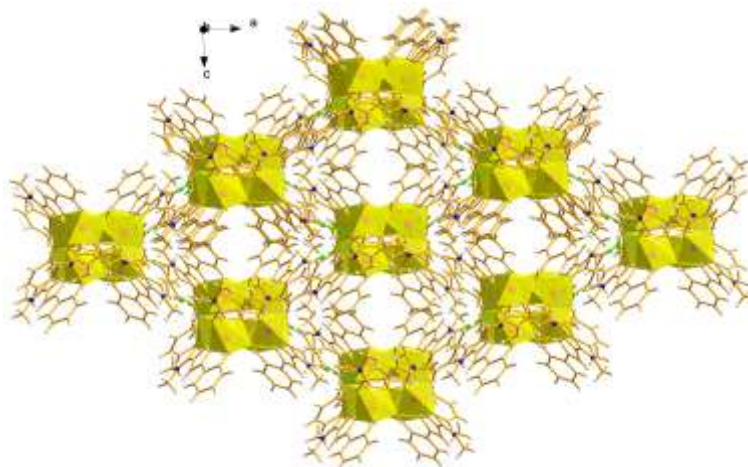


Fig. S5. Three-dimensional framework via supramolecular interactions of complex **3**.

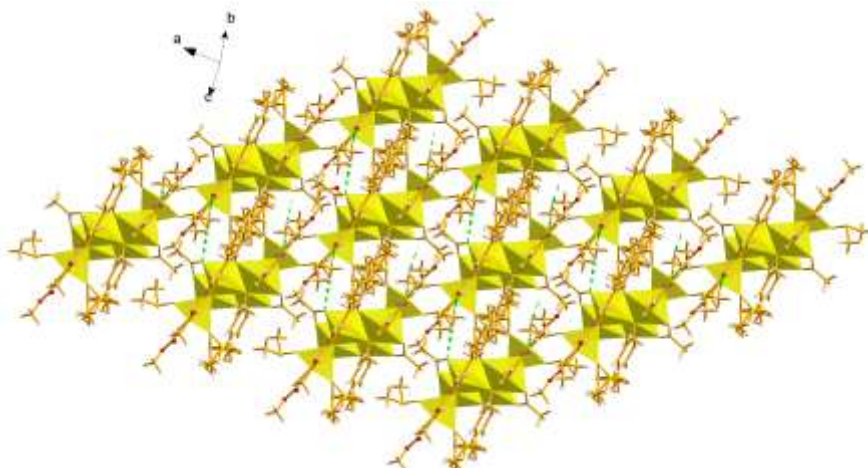


Fig. S6. Two-dimensional framework via supramolecular interactions of complex **5**.

Table S1. Selected bond distances (Å) and angles (°) for complex **1–3** and **5**.

1		2	
Mn(1)-O(3)#1	1.8432(16)	Mn(1)-O(3)	1.842(3)
Mn(1)-O(1)	1.9547(15)	Mn(1)-O(1)	1.939(3)
Mn(1)-N(2)#1	1.9849(17)	Mn(1)-N(2)	1.967(3)
Mn(1)-N(1)	1.9977(18)	Mn(1)-N(1)	1.996(3)
Mn(1)-N(4)	2.355(2)	Mn(1)-O(5)	2.231(4)
Mn(1)-N(5)	2.368(2)	Mn(1)-O(4)	2.285(8)
O(3)#1-Mn(1)-O(1)	93.23(7)	O(3)-Mn(1)-O(1)	91.64(14)
O(3)#1-Mn(1)-N(2)#1	89.79(7)	O(3)-Mn(1)-N(2)	90.49(14)
O(1)-Mn(1)-N(1)	81.55(7)	O(1)-Mn(1)-N(1)	81.16(13)
N(2)#1-Mn(1)-N(1)	95.54(7)	N(2)-Mn(1)-N(1)	96.80(13)
O(3)#1-Mn(1)-N(4)	87.57(7)	O(3)-Mn(1)-O(5)	90.9(2)
O(1)-Mn(1)-N(4)	89.10(7)	O(1)-Mn(1)-O(5)	88.34(16)
N(2)#1-Mn(1)-N(4)	92.73(7)	N(2)-Mn(1)-O(5)	89.27(16)
N(1)-Mn(1)-N(4)	88.84(7)	N(1)-Mn(1)-O(5)	91.29(17)
O(3)#1-Mn(1)-N(5)	89.86(8)	O(3)-Mn(1)-O(4)	95.9(3)
O(1)-Mn(1)-N(5)	83.73(7)	O(1)-Mn(1)-O(4)	91.3(2)
N(2)#1-Mn(1)-N(5)	94.59(7)	N(2)-Mn(1)-O(4)	90.9(2)
N(1)-Mn(1)-N(5)	93.03(7)	N(1)-Mn(1)-O(4)	81.9(2)
3			
Mn(1)-O(3)#1	1.877(4)	Mn(1)-N(2)	2.012(5)
Mn(1)-O(1)	1.883(5)	Mn(1)-O(3)	2.150(4)
Mn(1)-N(1)	1.990(5)	Mn(1)-O(2)	2.406(5)
O(3)#1-Mn(1)-N(1)	85.5(2)	O(1)-Mn(1)-N(1)	87.7(2)
O(3)#1-Mn(1)-N(2)	89.98(19)	O(1)-Mn(1)-N(2)	96.8(2)
O(3)#1-Mn(1)-O(3)	91.9(2)	O(1)-Mn(1)-O(3)	90.1(2)
N(2)-Mn(1)-O(3)	78.9(2)	O(3)#1-Mn(1)-O(2)	95.88(19)
O(1)-Mn(1)-O(2)	85.7(2)	N(2)-Mn(1)-O(2)	70.3(2)
5			
Mn(1)-O(10)	1.808(8)	Mn(1)-O(6)	1.833(8)
Mn(1)-N(6)	1.925(10)	Mn(1)-O(9)	1.957(7)
Mn(1)-O(7)	2.127(9)	Mn(1)-O(3)	2.574(5)
Mn(2)-O(10)#1	1.796(7)	Mn(2)-O(3)	1.877(7)
Mn(2)-N(3)	1.955(10)	Mn(2)-O(9)#1	1.974(8)
Mn(2)-O(8)#1	2.123(9)	Mn(2)-O(9)	2.332(8)
Mn(3)-O(10)	2.069(8)	Mn(3)-O(11)	2.080(9)
Mn(3)-O(12)	2.111(9)	Mn(3)-N(2)#1	2.182(10)
Mn(3)-N(5)	2.212(11)	Mn(3)-O(1)	2.812(3)
Mn(1)-Mn(2)#1	2.813(3)	Mn(2)-Mn(1)#1	2.813(3)
O(10)-Mn(1)-N(6)	91.0(4)	O(6)-Mn(1)-N(6)	89.4(4)
O(10)-Mn(1)-O(9)	81.1(3)	O(6)-Mn(1)-O(9)	98.0(3)
O(10)-Mn(1)-O(7)	92.4(4)	O(6)-Mn(1)-O(7)	91.3(4)
N(6)-Mn(1)-O(7)	99.1(4)	O(9)-Mn(1)-O(7)	89.9(3)

O(10)#1-Mn(2)-N(3)	89.4(4)	O(3)-Mn(2)-N(3)	90.0(4)
O(10)#1-Mn(2)-O(9)#1	80.9(3)	O(3)-Mn(2)-O(9)#1	98.9(3)
O(10)#1-Mn(2)-O(8)#1	94.2(3)	O(3)-Mn(2)-O(8)#1	94.9(3)
N(3)-Mn(2)-O(8)#1	96.6(4)	O(9)#1-Mn(2)-O(8)#1	88.5(3)
O(10)#1-Mn(2)-O(9)	89.4(3)	O(3)-Mn(2)-O(9)	81.6(3)
N(3)-Mn(2)-O(9)	97.6(4)	O(9)#1-Mn(2)-O(9)	78.1(3)
O(10)-Mn(3)-N(2)#1	80.1(3)	O(11)-Mn(3)-N(2)#1	92.3(4)
O(12)-Mn(3)-N(2)#1	94.4(4)	O(10)-Mn(3)-N(5)	79.8(3)
O(11)-Mn(3)-N(5)	92.0(4)	O(12)-Mn(3)-N(5)	96.3(4)

Symmetry transformations used to generate equivalent atoms: Complex **1**, #1: -x+2, -y+1, -z+1; complex **2**, #1: -x+1, -y+1, -z; Complex **3**, #1: x+1/4, -y+5/4, -z+1/4; #2: -x+5/4, y-1/4, -z+1/4; Complex **5**, #1: -x, -y, -z.

Table S2. The supramolecular interactions in complexes **1–5**.

complex 1			
	H...O(Å)	C-H...O(Å)	∠C-H...O(°)
C3-H3...O2	2.556	3.457	163.3
C17-H17...O1	2.615	3.436	147.5
C13-H13...O2	2.506	3.205	132.3
Complex 2			
C8-H8...O2	2.668	3.590	171.0
C3-H3...O2	2.401	3.278	156.9
Complex 3			
C11-H11B...O2	2.633	3.584	171.3
C11-H12B...O2	2.702	3.630	162.9
C12-H12C...O1	2.574	3.331	136.1
Complex 5			
C27-H27A...O2	2.556	3.501	167.9
C27-H27C...O8	2.581	3.509	163.1

Table S3. BVS calculations for the complexes 1-5.

		Mn ²⁺	Mn ³⁺	Mn ⁴⁺
Complex 1	Mn(1)	3.435722	3.168145	3.10877
Complex 2	Mn(1)	3.552557	3.27588	3.214486
Complex 3	Mn(1)	3.509644	3.236309	3.175657
Complex 4	Mn(1)	3.309456	3.051712	2.994519
	Mn(2)	2.215938	2.043359	2.005064
	Mn(3)	2.177418	2.007838	1.970209
	Mn(4)	3.339875	3.079762	3.022044
Complex 5	Mn(1)	3.845362	3.545881	3.479427
	Mn(2)	3.797979	3.502188	3.436553
	Mn(3)	2.219678	2.046807	2.008447

(1) I. D. Brown and D. Altermatt, *Acta Cryst.*, **B41**, 244.

(2) H. H. Thorp, *Inorg. Chem.*, 1992, **31**, 1585.

(3) W. T. Liu and H. H. Thorp, *Inorg. Chem.*, 1993, **32**, 4102.

Theoretical Model for complex 3.

The complete spin Hamiltonian for complex **3** is given by Eq 1. $H = -2J(S_1S_2 + S_2S_3 + S_3S_4 + S_4S_1)$ (1). The spin state of complex **3** and magnetic exchange paths are given in Fig. S7.

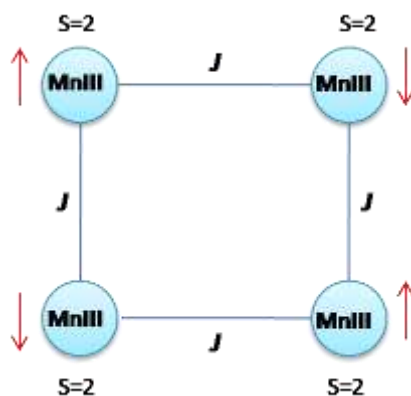


Fig. S7 The spin states of complex **3** and magnetic exchange paths

By use of the Kambe vector coupling method, with the total spin of the system defined as $S_A = S_1 + S_3$, $S_B = S_2 + S_4$, and $S_T = S_A + S_B$, the spin Hamiltonian can be transformed into that Eq. (2). $H = -J(S_T^2 - S_A^2 - S_B^2)$ (2). The corresponding expression of the relative energies is given in Eq. (3).

$$E(S_T, S_A, S_B) = -J[S_T(S_T+1) - S_A(S_A+1) - S_B(S_B+1)] \quad (3)$$

The molecule magnetic susceptibility expression in the van Vleck equation is given

below:

$$x = J/\kappa T;$$

N is Avogadro's number;

κ is Boltzmann constant;

β is Bohr magneton.

The analysis of the relative energies represents 84 states. If $J < 0$, the ground state is 0 with energy $E(0, 4, 4)$. Thus, the local spin can be obtained, and the spin coupling displayed antiferromagnetic interactions.

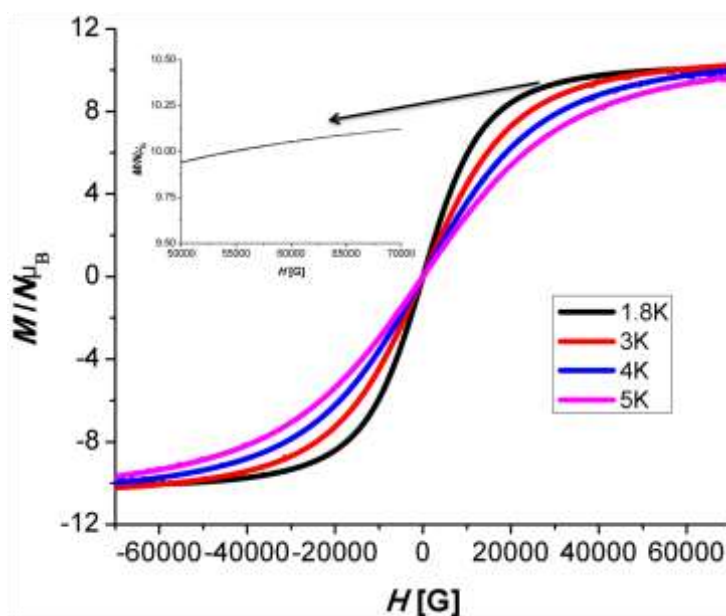


Fig. S8. Plots of isothermal magnetization M versus field H for complex 5 between 1.8–5 K.

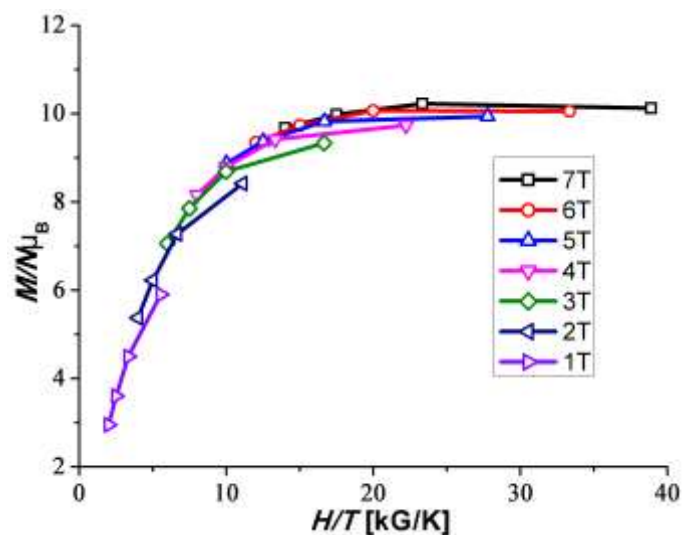


Fig. S9. Plots of reduced magnetization M versus H/T at the indicated applied fields.

The magnetic susceptibility of Complex 5

Analytical expression of the magnetic susceptibility for an $S = 2-2-5/2$ magnetic trimer in the low field is given as follow:

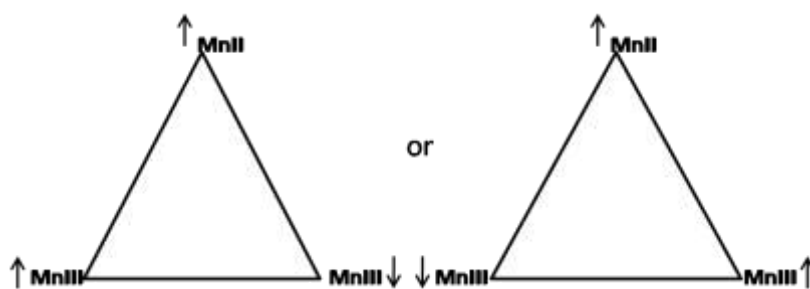


Fig. S10. The local spin in each triangular aza8-MC-3 subunit.